

Original Article

Designing Low-Consumption Code for Polarization-Multiplexed OCDMA Using AND -Subtraction Detection for Power-Efficient Metropolitan Networks

Chetan R Chauhan¹, Pravin R Prajapati²

¹Gujarat Technological University, Gujarat, India.

²A D Patel Institute of Technology, The Charutar Vidya Mandal (CVM) University,
New Vallabh Vidhyanagar, Gujarat, India.

¹Corresponding Author : chetan.svit@gmail.com

Received: 07 August 2025

Revised: 26 September 2025

Accepted: 12 October 2025

Published: 29 October 2025

Abstract - This paper presents a Low-Consumption Code integrated with polarization-multiplexed SAC-OCDMA and AND-subtraction detection to address the demand for energy-efficient, high-capacity optical networks. The proposed LCC, characterized by short code length and low cross-correlation derived from a diagonal matrix-based design, reduces interference, simplifies signal recovery, and lowers transmission power requirements. Analytical results show that the system supports up to 146 users, a 61% increase over conventional MD code systems, while maintaining a BER below 10^{-9} . The use of AND-subtraction detection enhances system scalability. It provides a 10.6% increase in user capacity by improving interference suppression and detection accuracy compared to the existing ZCC-coded system. The system also exhibits strong sensitivity to receiver effective power. The receiver power increases from -15 dBm to -10 dBm, and the number of users that can connect simultaneously rises from 118 to 156. Using orthogonal polarization states to improve energy efficiency, polarization multiplexing boosts spectral efficiency and lowers transmission power. In general, these results show that the LCC-coded PM-SAC-OCDMA architecture is a scalable and power-efficient option for next-generation metropolitan optical networks. It has more capacity, uses less energy, and operates reliably.

Keywords - AND Subtraction Detection, Low Consumption Code, Optical Code Division Multiple Access, Polarization Multiplexing.

1. Introduction

As the amount of data flow throughout the world continues to increase rapidly, energy efficiency has become a very important issue in the design of modern communication networks. Optical networks must meet the dual challenge of increasing data demands while minimizing energy consumption [1]. A fundamental problem is making communication systems more spectrally efficient, which means using bandwidth more effectively [2]. In Optical Code Division Multiple Access (OCDMA) networks, Spectral Amplitude Coding OCDMA (SAC-OCDMA) is an effective technique for augmenting network capacity [2], [3]. However, it is still hard to improve spectral efficiency without using more power. To make SAC-OCDMA energy-efficient, codes that save power and reduce interference must be devised. These codes also need to employ optical resources optimally [5].

SAC-OCDMA supports multiple users in sharing the same optical medium. It allocates each user a unique code [3].

This multiplexing technique uses spectral amplitude modulation to separate user signals. The orthogonal or low cross-correlation codes allow multiple users to transmit data simultaneously without interference. Existing SAC-OCDMA systems, based on Zero Cross-Correlation (ZCC) and Flexible Cross-Correlation (FCC) codes [9], [10], [14] encounter significant challenges. ZCC codes reduce Multiple Access Interference (MAI) but require long code lengths. It increases latency and reduces efficiency [12]. FCC codes are shorter but produce higher cross-correlation. Higher cross-correlation leads to increased interference [14]. In addition, conventional SAC-OCDMA designs use high-weight codes and complex detection techniques. These limitations result in higher power consumption and reduced spectral efficiency. It also has fewer supported users in the system [6].

To address these challenges, this work introduces a novel Low Consumption Code (LCC) for SAC-OCDMA systems [17]. The LCC code is shorter and has low cross-correlation qualities. These features enable the system to use less power



and improve energy and spectrum efficiency. Its simple design further minimizes system complexity without compromising performance. The short-length, low cross-correlation properties of a code improve system BER efficiency and increase user capacity [18].

The proposed LCC code is compared with existing MD [10], ZCC [16], MND [13], and FCC [14] codes under identical conditions, showing superior performance in power efficiency and spectral utilization. Also, polarization multiplexing is introduced to transmit data through orthogonal polarization states. It further enhances the spectral efficiency and, consequently, the total user capacity.

The AND subtraction detection method is employed to further improve signal recovery and reduce MAI [3], [6]. Optical fibers often face polarization dispersion. Using polarization multiplexing with LCC coding helps overcome this challenge. This approach enables energy-efficient and high-capacity SAC-OCDMA systems for next-generation metropolitan optical networks. [16].

2. LCC Code Construction Algorithm

The LCC is made up of two main parts: the data matrix (D) and code matrix (C) [9]. The data segment uses a diagonal matrix of size $K \times K$. Term K represents the total number of users. This matrix is repeated twice to properly align with the users. These matrices maintain zero cross-correlation at the receiver end. The signal is easily recovered due to zero cross-correlation at the receiver end. This design also reduces the need for high code weights, even with many users in the system. The reduced code weight requirement lowers the power consumption in the system. $K \times K$ can represent the Data Segment for $K=4$ and $W=4$ repeated for 2 times

$$[D] = \begin{bmatrix} 1 & 0 & 0 & 0 & 1 & 0 & 0 & 0 \\ 0 & 1 & 0 & 0 & 0 & 1 & 0 & 0 \\ 0 & 0 & 1 & 0 & 0 & 0 & 1 & 0 \\ 0 & 0 & 0 & 1 & 0 & 0 & 0 & 1 \end{bmatrix}$$

The Code Segment is created by using several smaller diagonal matrices (M). Each matrix is of size $(K/2) \times (K/2)$. These matrices are repeated horizontally ($W-2$) times and once vertically to form the full code segment.

$$[C] = \begin{bmatrix} 1 & 0 & 1 & 0 \\ 0 & 1 & 0 & 1 \\ 1 & 0 & 1 & 0 \\ 0 & 1 & 0 & 1 \end{bmatrix}$$

This design assigns each base station a unique row from the matrix as its code sequence. It helps maintain efficient data transmission and keeps power consumption low. For $K=4$ and $W=4$, diagonal matrix of size $(K/2) \times (K/2) = 2 \times 2$. This

matrix is repeated $(W-2) = 2$ times and then copied vertically. The constructed LCC code is derived as follows.

$$[G] = \begin{bmatrix} 1 & 0 & 0 & 0 & 1 & 0 & 0 & 0 & 1 & 0 & 1 & 0 \\ 0 & 1 & 0 & 0 & 0 & 1 & 0 & 0 & 0 & 1 & 0 & 1 \\ 0 & 0 & 1 & 0 & 0 & 0 & 1 & 0 & 1 & 0 & 1 & 0 \\ 0 & 0 & 0 & 1 & 0 & 0 & 0 & 1 & 0 & 1 & 0 & 1 \end{bmatrix}$$

With a code weight of 4, the user base station selects its code from a specific row in the matrix, which is $[1 \ 0 \ 0 \ 0 \ 1 \ 0 \ 0 \ 0 \ 1 \ 0 \ 1 \ 0]$. The total code length (N) is calculated as $(K \times 2) + (K/2 \times (W-2))$. It ensures a compact design to save bandwidth and power requirements. In SAC encoding, the base station transmits on wavelengths at $[\lambda_1, \lambda_5, \lambda_9, \lambda_{11}]$. Each wavelength represents bit 1's [5], which modulates the signal on these optical wavelengths. The LCC is designed so that only $W-2$ bits are cross-correlated with one base station user. All other users remain unaffected in the system. The LCC also uses two diagonal matrices, making it easier to detect the signal. This approach makes it possible to design codes with smaller code weights. It increases the number of supported users and lowers the overall power consumption of the system. So, LCC code design uses less energy per unit of time. By minimizing cross-correlation between codes, detection becomes more efficient.

2.1. System Flow Diagram

Data of each user is modulated over a polarization split encoded data at the transmitter end. The system diagram is reflected in Figure 1. An optical broadband light source is first polarization split. User 1 modulates its electrical signal using a Mach-Zehnder Modulator (MZM) on the X-polarized light beam, while user 2 modulates its data onto the Y-polarized light beam. The polarization split optical beam is spectrally amplitude-coded using the LCC code. If User 1 is assigned the code sequence "1 0 0 0 1 0 1," the X-polarized light beam will encode data onto the wavelengths corresponding to the positions of '1' in the sequence. In this case, data is encoded on the λ_1, λ_5 , and λ_7 .

The polarization combiner combines the modulated encoded beams from both users and transmits them through the optical cable. At the receiver end, the data is first split by polarization. The X-polarization data is passed through a decoder and recovered by a PIN detector. The recovered signal is then AND-subtracted with the filtered wavelengths from other users [3]. The access power is caused by cross-correlation, which minimizes interference between the signals through this process. Finally, the recovered signal is reshaped and forwarded to a BER analyzer for comparison. The LCC for polarization-multiplexed OCDMA systems is made to use less power while yet being able to handle many users. The design of the LCC for polarization-multiplexed OCDMA systems focuses on reducing power consumption while supporting many users.

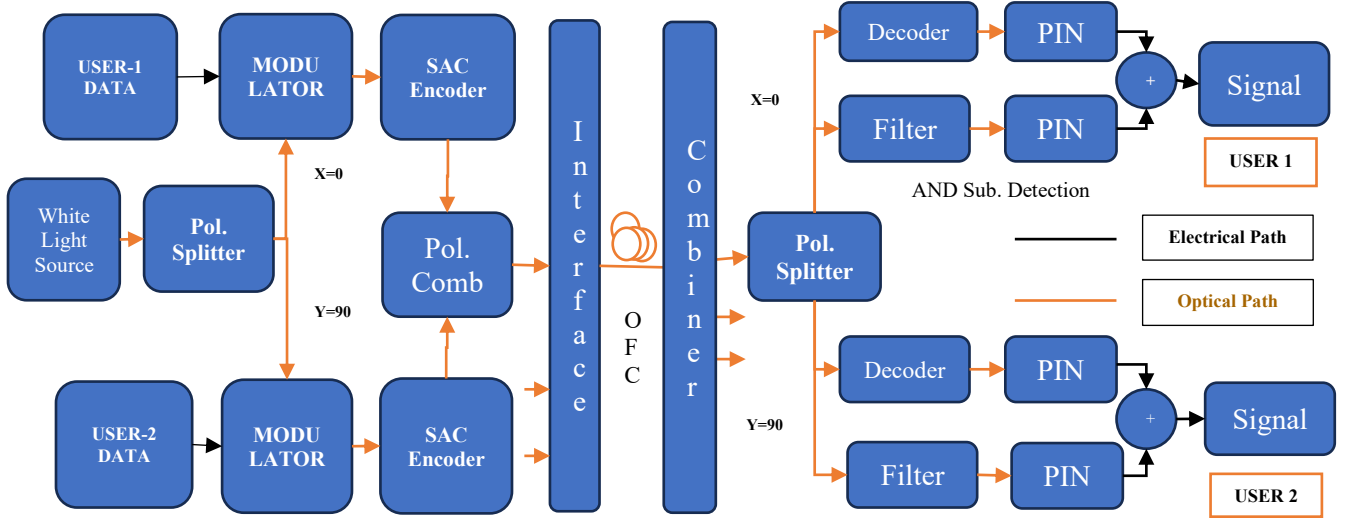


Fig. 1 LCC code SAC-OCDMA system flow diagram

When many individuals are using the network, important metrics like Signal-to-Noise Ratio (SNR) can be used to show how well the system functions [13], [14]. The Bit-Error-Rate (BER) derived from SNR indicates how many users the system can support. The SNR [9], [14] is written as:

$$SNR = \frac{\langle I^2 \rangle}{\langle \sigma^2 \rangle} = \frac{\langle I_p^2 \rangle}{\langle I_{sh}^2 \rangle + PIIN + \langle I_{th}^2 \rangle} \quad (1)$$

I_{sh}^2 demonstrates the strength of shot noise, a fundamental source of noise in optical communication systems. PIIN stands for Phase-Induced Intensity Noise, which happens when signal phases interact in polarization multiplexing.

I_{th}^2 is the same as thermal noise, which is caused by the random movement of charge carriers in electronic parts. A spectral density function $g(v)$ describes the received signal. It shows how the strength of the signal is spread out across the frequency spectrum.

$$I = I_1 - I_2 = \Re \int_0^\infty G_1(v) dv - \Re \int_0^\infty G_2(v) dv \quad (2)$$

The photodetector's responsivity is denoted by \Re [12]. The Gaussian approximation is employed as the analytical framework to assess system performance [8]. The photocurrent of the detector is used to calculate the SNR at the receiver. The analysis considers the combined effects of thermal noise (σ_{th}), shot noise (σ_{sh}), and PIIN (σ_{PIIN}) noise [9]. PSD is expressed as below during a single bit interval [13].

$$\int_0^\infty G_1(v) dv = \int_0^\infty \left[\frac{P_{sr}}{v} \sum_{k=1}^K d_k \sum_{i=1}^N c_k(i) c_l(i) \text{rect}(i) \right] \quad (3)$$

P_{sr} denotes the effective received power at the receiver end. It is measured at the output of the optical fiber cable [15], [16]. The LCC code employs the following cross-correlation formulation.

$$\sum_{i=1}^N p_m(i) p_l(i) = \begin{cases} W, \text{form} = l \\ (W-2), \text{for} \begin{cases} l = m + (K/2), \text{if } m > l \\ l = l - (K/2), \text{if } l > m \end{cases} \\ 0, \text{else} \end{cases} \quad (4)$$

$$\sum_{i=1}^N p_{mT}(i) p_m(i) p_l(i) = \begin{cases} W-2, \text{form} = l \\ mT, \text{for} \begin{cases} mT = k + (K/2), \text{if } m > mT \\ mT = l - (K/2), \text{if } mT > m \end{cases} \\ 0, \text{otherwise} \end{cases} \quad (5)$$

N is the total length of the LCC. The Power Spectral Density (PSD) corresponding to the i^{th} receiver in a polarization-multiplexed LCC-coded SAC-OCDMA system is formulated as follows. This representation describes the optical signal as detected by the PIN photodetector. [11].

$$I_1 = \Re \int_0^{+\infty} G_1(v) dv = \left[\Re \frac{P_{sr}}{L} \sum_{k=1}^K dk \sum_{i=1}^N p_m(i) \cdot p_l(i) \right] \cos \theta + \left[\Re \frac{P_{sr}}{L} \sum_{k=1}^K dk \sum_{i=1}^N p_m(i) \cdot p_l(i) \right] \sin \theta \quad (6)$$

It is assumed that all transmitters are sending the bit '1'. After the optical polarization is split at the receiver, the signal is ideally received. In this condition, $\sin \theta = 0$. Putting Equations 4 and 5 in Equation 6, we get the photodetector current as:

$$I_1 = \Re \left[\frac{P_{sr}}{L} \sum_{k=1}^K dk \sum_{i=1}^L p_m(i) \cdot p_l(i) \right] \cos \theta$$

$$I_1 = \Re \frac{P_{sr}}{N} (W + W - 2) = \Re \frac{2P_{sr}}{N} (W - 2) \quad (7)$$

The photodetector's responsivity (\Re) is given by $\Re = \eta e \lambda / hc$ [5]. The AND logic filtered interference signal is represented as:

$$I_2 = \left[\Re \frac{P_{sr}}{L} \sum_{k=1}^K dk \sum_{i=1}^N p_{mT}(i) p_m(i) \cdot p_l(i) \right] \cos \theta + \left[\Re \frac{P_{sr}}{L} \sum_{k=1}^K dk \sum_{i=1}^N p_{mT}(i) p_m(i) \cdot p_l(i) \right] \sin \theta$$

The recovered signal is mentioned as

$$I = I_1 - I_2 = \Re \frac{P_{sr}}{N} W \quad (8)$$

The shot noise at the receiver is derived through system analysis and is expressed as:

$$\sigma_{sh}^2 = 2eB(I_1 + I_2) = 2eB \Re \frac{P_{sr}}{N} (3W - 4) \quad (9)$$

Evaluating the Phase-Induced Intensity Noise (PIIN) [8],

$$\sigma_{PIIN}^2 = I^2 B \tau_c = B \Re \frac{2P_{sr}^2 K}{N^2 \Delta v} (3W - 4) \quad (10)$$

The thermal noise at the receiver end can be denoted as [6, 16]

$$\sigma_{th}^2 = \frac{4B_e K_B T_n}{R_L} \quad (11)$$

Here, B_e represents the electrical bandwidth and K_B is Boltzmann's constant. T_n denotes the receiver temperature, and R_L is the load resistance. The total noise is denoted as $\sigma^2 = \sigma_{sh}^2 + \sigma_{th}^2 + \sigma_{PIIN}^2$. The SNR can be calculated using equations 9, 10, and 11 as below

$$SNR = \frac{I^2}{\sigma^2} = \frac{\left(\Re \frac{P_{sr} W}{N} \right)^2}{2eB I + \frac{4K_B T_n B}{R_L} + I^2 B \tau_c} \quad (12)$$

The BER at the receiver is represented by

$$BER = 0.5 \operatorname{erf}(\sqrt{SNR}) \quad (13)$$

3. Simulation Model and Results

Figure 2 presents the system's simulation model. The signal is recovered at the receiver end, and the model is made for eight users.

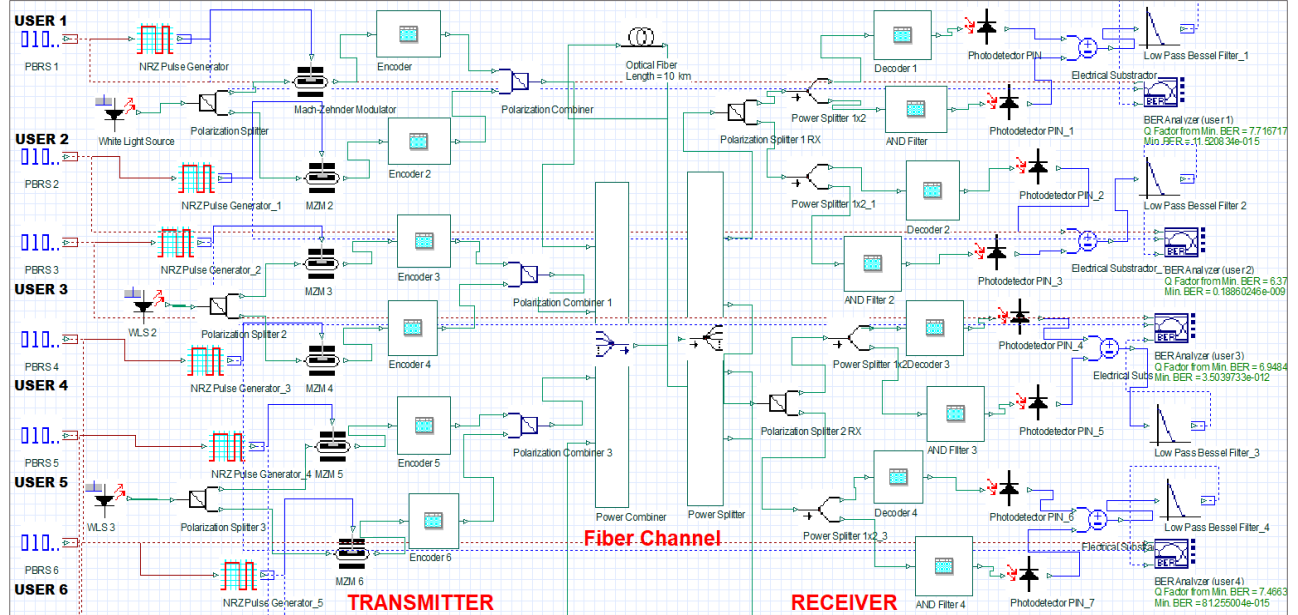


Fig. 2 Simulation model of the system

To modulate the input data using a polarization splitter, two users share a white light source centred at 1550.75 nm. A fiber Bragg grating-based encoder is used to encode the polarized signal. The polarization combiner combines the two optical beams. A single-mode optical fiber is then used to transmit the signal. The fiber has a differential group delay

of 0.2 ps/km and an attenuation of 0.2 dB/km. Another fiber Bragg grating is used to decode the data at the receiver end. A PIN photodetector detects the decoded signal. The signal is subsequently filtered using a low-pass Bessel filter to suppress unwanted noise. A BER analyzer then analyses it.

Figure 3(a) illustrates the eye diagram of the recovered signal for User 1 after transmission over 10 km of optical fiber. Figure 3(b) presents the corresponding eye diagram after 45 km. Reliable signal recovery is maintained up to 55 km, beyond which the BER exceeds 10^{-9} .

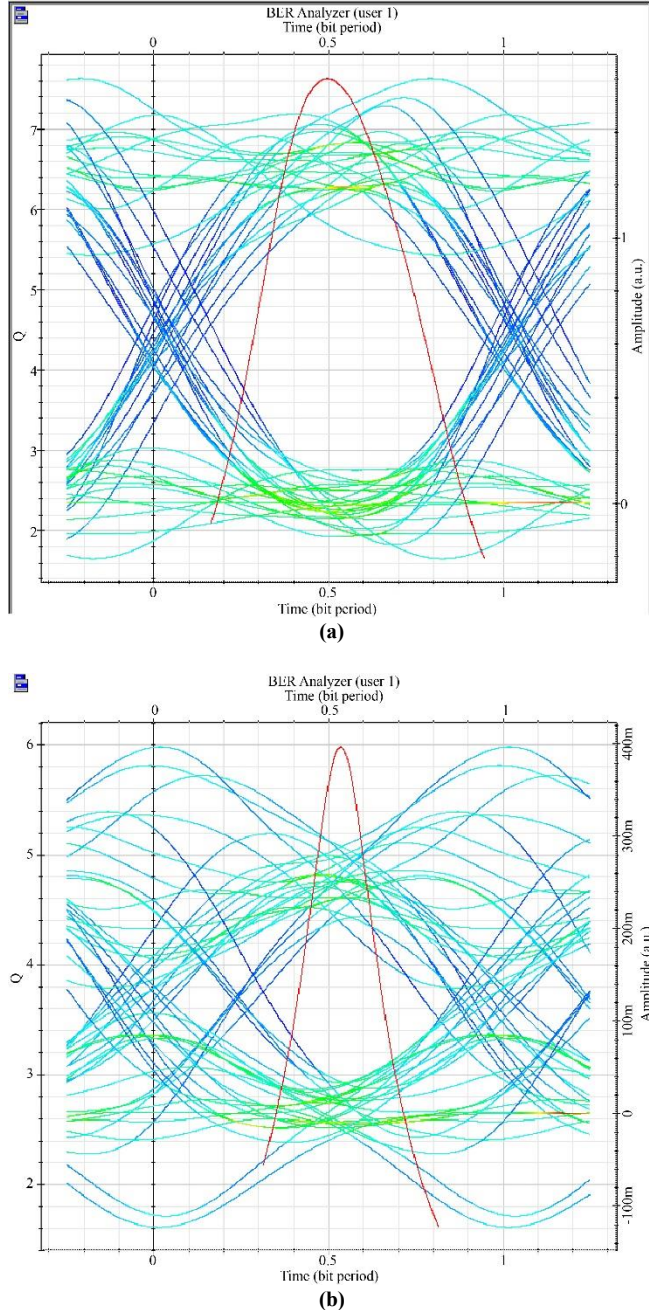


Fig. 3 Eye diagram of recovered signal (a) at 10 km (b) at 45 km for user 1

4. Results and Analysis

The performance of the LCC-based polarization-multiplexed OCDMA system is assessed and compared with conventional schemes, including FCC code [14], MD code

[10], MND code, and MDW code [13]. The key parameters employed for this evaluation are listed in Table 1.

Table 1. Typical system parameters

Parameters	Values
Operating Frequency	193.1 THz
Electrical Bandwidth (B_e)	311 MHz
Linewidth Source ($\Delta\nu$)	3.75 THz
Photodetector Quantum Eff. (η)	0.6
Bit Rate	622 Mbps
Receiver Noise Temp (T_n)	300 K
Receiver Load Resistor (R_L)	1030 Ω
Boltzmann's constant (K_b)	6.66×10^{-34} Js
Planck's constant (h)	1.38×10^{-23} J/K
Electron charge (e)	1.6×10^{-19} C

As shown in Figure 4, the LC-coded PM-OCDMA system supports 146 users, which is 61% more than the conventional MD code systems with a code weight of $W = 4$.

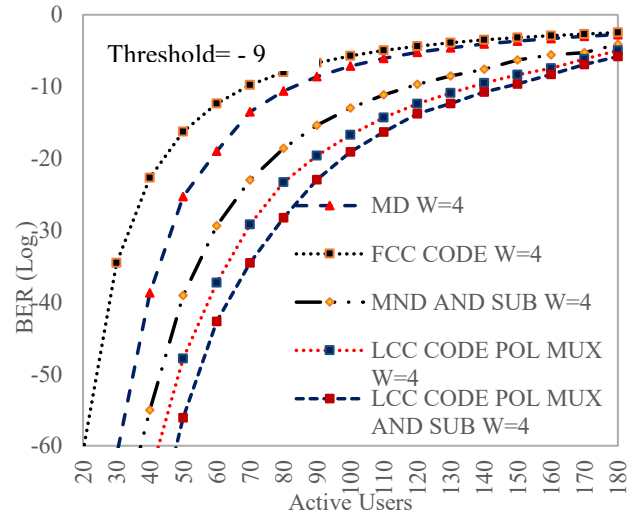


Fig. 4 BER vs Active users for different code systems

The system exhibits a prominent increase in user capacity through polarization multiplexing, which increases polarization-induced interference noise (PIIN). Performance is further enhanced by using AND subtraction detection. This technique increases the user capacity to 156 users. Compared to the ZCC code system under identical conditions, the LCC code boosts overall capacity by 10.6%. Thus, the LCC code improves system scalability while keeping BER low.

In terms of power efficiency, the LCC exhibits notable advantages. As illustrated in Figure 5, the BER decreases significantly as the receiver's effective power (P_{sr}) increases. When the receiver power rises from -15 dBm to -10 dBm, the system's user capacity expands from 118 to 156 users. It is proving that the system is sensitive to power. The LCC also benefits from a short code length and a low cross-correlation. It cuts down on interference and uses less power.

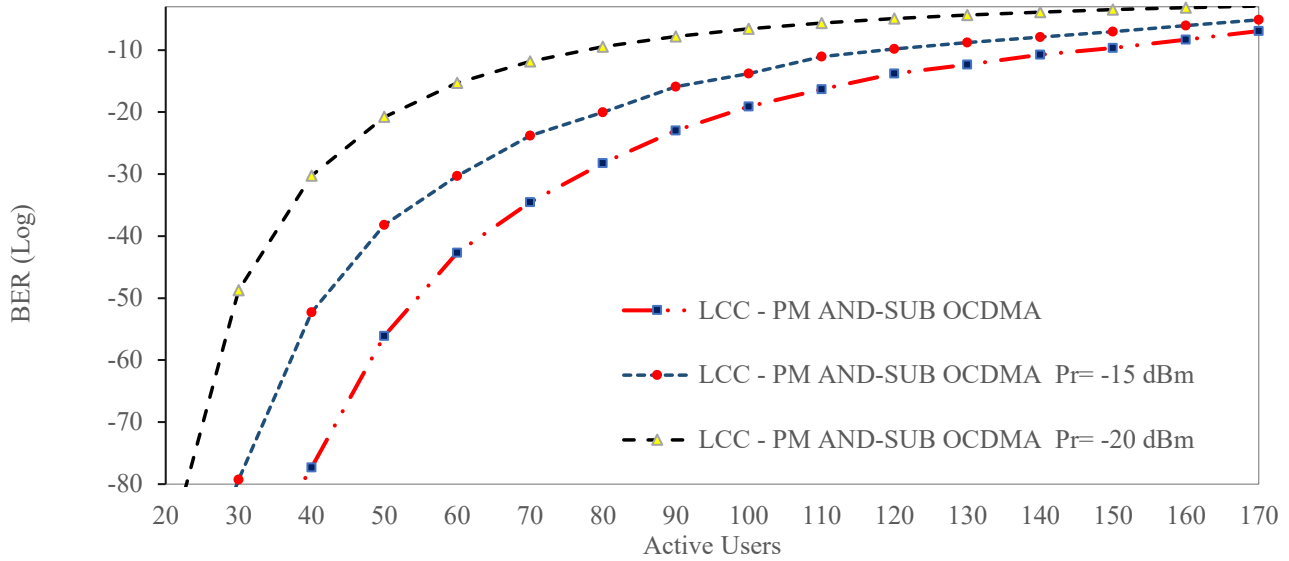


Fig. 5 BER vs Active users for the LCC LCC-coded system for different receiver powers

Two diagonal matrices are used to construct the code. This simplifies signal recovery at the receiver end and reduces power consumption. The power transmission requirement is effectively cut in half by polarization multiplexing, which makes this system ideal for energy-efficient optical networks. These findings show that the LCC-coded PM-OCDMA system performs better than conventional systems. It provides scalability, lower power consumption, and increased capacity for metropolitan optical communication networks.

5. Conclusion

The proposed Low Consumption Code (LCC) with polarization multiplexed SAC-OCDMA and AND subtraction detection shows clear improvements. It offers better scalability, higher power efficiency, and greater reliability. According to the analysis, the system can support up to 156 users. This is 61% greater than regular MD coding

systems, yet the BER stays below 10^{-9} . Adding AND-subtraction detection boosts capacity by 10.6%, reducing interference and enhancing detection accuracy.

The system is also quite sensitive to the effective power of the receiver. When the receiver power increases from -15 dBm to -10 dBm, the user capacity improves from 118 to 156 users. This shows that the LCC performs efficiently under different power conditions. The short code length and low cross-correlation of LCC simplify the receiver design and reduce power consumption. Polarization multiplexing further cuts transmission power in half by using orthogonal states. Overall, the obtained results demonstrate that the LCC-coded PM-OCDMA framework is a strong candidate for next-generation metropolitan optical networks. It provides high capacity, improved energy efficiency, and scalable performance.

References

- [1] Chih-Ta Yen, and Wen-Bin Chen, "A Study of Dispersion Compensation of Polarization Multiplexing-Based OFDM-OCDMA for Radio-Over-Fiber Transmissions," *Sensors*, vol. 16, no. 9, pp. 1-16, 2016. [\[CrossRef\]](#) [\[Google Scholar\]](#) [\[Publisher Link\]](#)
- [2] I.B. Djordjevic, and B. Vasic, "Combinatorial Constructions of Optical Orthogonal Codes for OCDMA Systems," *IEEE Communications Letters*, vol. 8, no. 6, pp. 391-393, 2004. [\[CrossRef\]](#) [\[Google Scholar\]](#) [\[Publisher Link\]](#)
- [3] Feras N. Hasoon et al., "Spectral Amplitude Coding OCDMA using and Subtraction Technique," *Applied Optics*, vol. 47, no. 9, pp. 1263-1268, 2008. [\[CrossRef\]](#) [\[Google Scholar\]](#) [\[Publisher Link\]](#)
- [4] Walid Sahraoui et al., "A Novel 2D Polarization-Spatial Encoding Approach for OCDMA System Based on Multi-Core Fiber," *Optik*, vol. 228, 2021. [\[CrossRef\]](#) [\[Google Scholar\]](#) [\[Publisher Link\]](#)
- [5] Syed Mohammad Ammar et al., "Development of New Spectral Amplitude Coding OCDMA Code by Using Polarization Encoding Technique," *Applied Sciences*, vol. 13, no. 5, pp. 1-15, 2023. [\[CrossRef\]](#) [\[Google Scholar\]](#) [\[Publisher Link\]](#)
- [6] Somia A. Abd El-Mottaleb et al., "An Efficient SAC-OCDMA System Using Three Different Codes and Two Different Detection Techniques," *Optical and Quantum Electronics*, vol. 51, no. 354, 2020. [\[CrossRef\]](#) [\[Google Scholar\]](#) [\[Publisher Link\]](#)
- [7] Teena Sharma, Ravi Kumar Maddila, and Syed Alwee Aljunid, "Simulative Investigation of Spectral Amplitude Coding Based OCDMA System Using Quantum Logic Gate Code with NAND and Direct Detection Techniques," *Current Optics and Photonics*, vol. 3, no. 6, pp. 531-540, 2019. [\[CrossRef\]](#) [\[Google Scholar\]](#) [\[Publisher Link\]](#)

- [8] Nabiha Jellali, Moez Ferchichi, and Monia Najjar, "4D Encoding Scheme for OCDMA System Based on Multi-Diagonal Code," *Optik*, vol. 244, 2021. [[CrossRef](#)] [[Google Scholar](#)] [[Publisher Link](#)]
- [9] Hichem Mrabet et al., "Nonlinear Effect and MAI Impact on SAC-OCDMA System Based on 2D Multi-Diagonal Code and Laser Array," *Applied Sciences*, vol. 11, no. 18, pp. 1-17, 2021. [[CrossRef](#)] [[Google Scholar](#)] [[Publisher Link](#)]
- [10] S.A. Aljunid et al., "A New Family of Optical Code Sequences for Spectral-Amplitude-Coding Optical CDMA Systems," *IEEE Photonics Technology Letters*, vol. 16, no. 10, pp. 2383-2385, 2004. [[CrossRef](#)] [[Google Scholar](#)] [[Publisher Link](#)]
- [11] Ahmed Garadi et al., "Enhanced Performances of SAC-OCDMA System by Using Polarization Encoding," *Journal of Optical Communications*, vol. 41, no. 3, pp. 319-324, 2020. [[CrossRef](#)] [[Google Scholar](#)] [[Publisher Link](#)]
- [12] Thanaa Hussein Abda et al., "Modeling and simulation of Multi Diagonal code with zero cross correlation for SAC-OCDMA networks," *2nd International Conference on Photonics*, Kota Kinabalu, Malaysia, pp. 1-5, 2011. [[CrossRef](#)] [[Google Scholar](#)] [[Publisher Link](#)]
- [13] N. Ahmed et al., "Performance Enhancement of OCDMA System using NAND Detection With Modified Double Weight (MDW) Code For Optical Access Network," *Optik*, vol. 124, no. 13, pp. 1402-1407, 2020. [[CrossRef](#)] [[Google Scholar](#)] [[Publisher Link](#)]
- [14] C.B.M. Rashidi et al., "New Design of Flexible Cross Correlation (FCC) Code for SAC-OCDMA System," *Procedia Engineering*, vol. 53, pp. 420-427, 2013. [[CrossRef](#)] [[Google Scholar](#)] [[Publisher Link](#)]
- [15] Bedir Yousif, Ibrahim El. Metwally, and Ahmed Shaban Samra, "A Modified Topology Achieved in OFDM/SAC-OCDMA-Based Multi-Diagonal Code for Enhancing Spectral Efficiency," *Photonic Network Communications*, vol. 37, no. 1, pp. 90-99, 2019. [[CrossRef](#)] [[Google Scholar](#)] [[Publisher Link](#)]
- [16] Ammar Armghan et al., "Performance Analysis of Hybrid PDM-SAC-OCDMA Enabled FSO Transmission Using ZCC Codes," *Applied Sciences*, vol. 13, no. 5, pp. 1-14, 2023. [[CrossRef](#)] [[Google Scholar](#)] [[Publisher Link](#)]
- [17] Ganesh C. Sankaran, and Krishna M. Sivalingam, "ONU Buffer Reduction for Power Efficiency in Passive Optical Networks," *Optical Switching and Networking*, vol. 10, no. 4, pp. 416-429, 2013. [[CrossRef](#)] [[Google Scholar](#)] [[Publisher Link](#)]
- [18] Fábio R. Durand, and Bruno A. Angélico, "Increasing Energy Efficiency in OCDMA Network Via Distributed Power Control," *Journal of Microwaves, Optoelectronics and Electromagnetic Applications*, vol. 11, no. 1, pp. 39-55, 2012. [[CrossRef](#)] [[Google Scholar](#)] [[Publisher Link](#)]